Differential Recognition of Syk-Binding Sites by Each of the Two Phosphotyrosine-Binding Pockets of the Vav SH2 Domain

Chih-Hong Chen,[1*] Dan Piraner,[1†] Nina M. Gorenstein,[2] Robert L. Geahlen,[1] Carol Beth Post[1,2,3]

[1] *Department of Medicinal Chemistry and Molecular Pharmacology, and Purdue Center for Cancer Research, Purdue University, West Lafayette, IN 47907*

[2] *Department of Biological Sciences, Purdue University, West Lafayette, IN 47907*

[3] *Markey Center for Structural Biology, Purdue University, West Lafayette, IN 47907*

Received 26 July 2013; revised 26 July 2013; accepted 6 August 2013
Published online 17 August 2013 in Wiley Online Library (wileyonlinelibrary.com). DOI 10.1002/bip.22371

ABSTRACT:

The association of spleen tyrosine kinase (Syk), a central tyrosine kinase in B cell signaling, with Vav SH2 domain is controlled by phosphorylation of two closely spaced tyrosines in Syk linker B: Y342 and Y346. Previous studies established both singly phosphorylated and doubly phosphorylated forms play a role in signaling. The structure of the doubly phosphorylated form identified a new recognition of phosphotyrosine whereby two phosphotyrosines bind simultaneously to the Vav SH2 domain, one in the canonical pTyr pocket and one in the specificity pocket on the opposite side of the central β-sheet. It is unknown if the specificity pocket can bind phosphotyrosine independent of phosphotyrosine binding the pTyr pocket. To address this gap in knowledge, we determined the structure of the complex between Vav1 SH2 and a peptide (SykLB-YpY) modeling the singly phosphorylated-Y346 form of Syk with unphosphorylated Y342. The nuclear magnetic resonance (NMR) data conclusively establish that recognition of phosphotyrosine is swapped between the two pockets; phosphorylated pY346 binds the specificity pocket of Vav1 SH2, and unphosphorylated Y342 occupies what is normally the pTyr binding pocket. Nearly identical changes in chemical shifts occurred upon binding all three forms of singly and doubly phosphorylated peptides; however, somewhat smaller shift perturbations for SykLB-YpY from residues in regions of high internal mobility suggest that internal motions are coupled to binding affinity. The differential recognition that includes this swapped binding of phosphotyrosine to the specificity pocket of Vav SH2 increases the repertoire of possible phosphotyrosine binding by SH2 domains in regulating protein-protein interactions in cellular signaling.
Biopolymers 99: 897–907, 2013.

Keywords: *phosphotyrosine recognition; internal dynamics coupled to affinity; intermolecular nuclear Overhauser effect; induced-fit binding; electrostatic potential surface*

Correspondence to: Carol Beth Post, Ph.D.; e-mail: cbp@purdue.edu
*Present address: City of Hope, Duarte, CA.
†Present address: Biochemistry and Molecular Biophysics, California Institute of Technology.
Contract grant sponsor: National Institutes of Health (NIH) (C.B.P.)
Contract grant number: R01-GM039478
Contract grant sponsor: National Institutes of Health (NIH) (R.L.G.)
Contract grant number: R01-AI098132
Contract grant sponsor: Purdue University Reinvestment
Contract grant sponsor: Purdue Center for Cancer Research
Contract grant number: P30-CA23168

This article was originally published online as an accepted preprint. The "Published Online" date corresponds to the preprint version. You can request a copy of the preprint by emailing the Biopolymers editorial office at biopolymers@wiley.com

INTRODUCTION

Spleen tyrosine kinase, Syk, is an essential component of the B cell signaling network to produce antigen-specific antibodies that target foreign molecules in the adaptive immune response.[1] The B cell receptor, BCR, recognizes foreign molecules and this engagement of the receptor leads to phosphorylation of the BCR intracellular tyrosine activation motif, ITAM, clustering of BCR molecules, activation of Syk, and enhanced levels of tyrosine phosphorylation of numerous intracellular proteins. Syk activation and phosphorylation on many tyrosines generates recognition sites allowing Syk to interact with various effector proteins and to participate in the formation of large signaling complexes at the clustered receptors. The Vav family of guanine nucleotide exchange factors, GEFs, is one such effector protein[2–4]; in addition to GEF activity, the Vav family acts as scaffolding proteins to promote the assembly of the signaling complexes[5] and is essential for B cell development.[6] As does Syk, Vav has multiple binding partners. The SH2 domain of Vav1 mediates its interaction with a wide variety of binding partners with disparate functionality, including kinases and phosphatases,[7,8] receptor proteins,[9] and several scaffolding proteins.[10–14] This wide diversity in molecular interactions suggests Vav SH2 recognition is multifaceted.

Syk associates with Vav through the SH2 domain of Vav and the linker B region of Syk connecting the two tandem SH2 domains and the catalytic domain. Syk linker B contains several tyrosines that are phosphorylated to regulate Syk binding to its multiple binding partners and to couple the BCR, as well as other ITAM-containing receptors, to alternative signaling pathways.[1] The highest proportion of phosphorylation in humans occurs at two of these linker B sites[15]: Y348 and Y352, equivalent to Y342 and Y346 in mouse (murine Syk numbering is used throughout this article), and Y315 and Y319 in Zap-70, which is the only other member of the Syk family of cytoplasmic tyrosine kinases and is expressed in T cells. Vav binds the region of Y342 and Y346, which in its doubly phosphorylated form is an unusual recognition site of two closely spaced phosphotyrosines that binds a single SH2 domain of certain Syk partners.[16]

SH2 domains comprise approximately 100 residues that fold independently into a central β-sheet flanked by two α-helices (Figure 1). Vav1 SH2 (protein data bank, PDB code 2CRH) has a nonaromatic hydrophobic Ile residue at the βD5 position, and therefore, belongs to the new group IIA in the classification[17] of the more than 100 SH2 domains in the human genome. The specificity derived from the proteins known to interact with Vav1 SH2 places proline at the pTyr +3 position.[7,9–14] This preference combined with the phosphopeptide screening[17] gives the sequence specificity pYΦXP where pY is phosphotyrosine, Φ is a hydrophobic amino acid, and X is any amino acid.

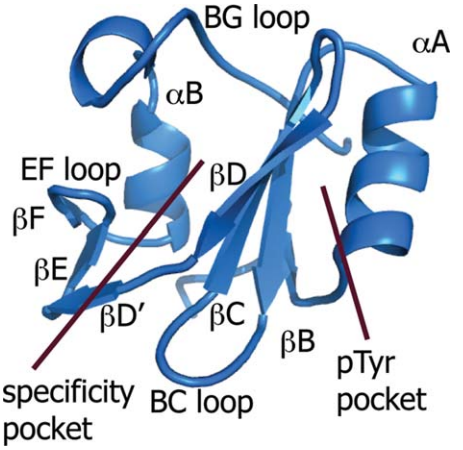

FIGURE 1 Ribbon diagram of the Vav1 SH2 structure indicating the regions of the specificity pocket and pTyr pocket on each side of the central β-sheet. The central β-sheet comprises βB, βC, and βD, and the secondary β-sheet comprises βD′, βE, and βF.

The canonical binding site of SH2 domains for phosphotyrosine lies on the side of the central β-sheet near αA (Figure 1). The phosphoryl group interacts with two highly conserved SH2 residues: RβB5 and HβD4.[18] It is generally thought that phosphotyrosine binding in this pTyr pocket provides as much as half of the free energy for binding; equilibrium binding constants for phosphorylated peptides are 10^3 to 10^4 higher affinity than the unphosphorylated peptide of the same sequence.[19–21] A second pocket on the opposite side of the central β-sheet, called the specificity pocket, has higher sequence variability as well as structural variation in the secondary β-sheet (βD′ to βF) and BG loop.[18] This pocket is the site associated with specific recognition of the SH2 domain for its binding partner and interacts with amino acids C-terminal to phosphotyrosine. Recognition determinants beyond these canonical binding interactions include binding contacts that extend N-terminal to phosphotyrosine,[22] phosphorylation-independent binding,[22,23] and simultaneous binding of two peptides.[24]

The Vav family SH2 domain recognizes the Syk linker B region spanning Y342 and Y346 with an affinity that depends on the phosphorylation state[25]; the doubly phosphorylated state with both pY342 and pY346 has highest affinity, and the singly phosphorylated states are two-fold lower for pY342 and 10-fold lower for pY346. Moreover, cellular response levels in B cell signaling match these relative binding affinities, which suggests that recognition of Y342/Y346 is a limiting factor in signaling. The unusual recognition of two closely spaced tyrosines by a single SH2 domain occurs by binding pY342 in the

canonical pTyr pocket and pY346 in the specificity pocket.[25] A similar binding orientation was determined for the interaction of the same doubly phosphorylated region of linker B with the C-terminal SH2 domain of phospholipase C-γ (PLC-γ),[16] another downstream target in B cell signaling. Here, we address the question of how is the singly phosphorylated pY346 form of Syk linker B recognized. Is the mode of binding with pY346 located in the specificity pocket sufficiently stable to be preferred over one with a change in orientation that positions the single phosphotyrosine in the canonical pTyr pocket? The preferred orientation is unclear at the outset given that the sequence C-terminal to both of these tyrosines, $Y_{342}ESPY_{346}ADP$, corresponds to the pYΦXP consensus sequence noted above, and that phosphotyrosine binding contributes half of the binding free energy in other SH2 domain interactions. Recent technological developments in high-throughput assay of cellular SH2-protein interactions allow a remarkable capability of detecting hundreds of potential functional associations, many of which were previously unknown.[26] This growing set of SH2 interactions emphasizes the need to expand our knowledge of the structural basis for SH2 mediated protein-protein interactions.

RESULTS

Chemical Shift Perturbation (CSP) to Monitor Syk Linker B Association with Vav1

The interaction of Syk with Vav1 SH2 is regulated by tyrosine phosphorylation of Syk linker B.[25] The effect of phosphorylation was examined using peptides derived from the Syk linker B sequence 338 to 353 ($DTEVY_{342}ESPY_{346}ADPE$) and containing phosphotyrosine at either position 342 (SykLB-pYY), 346 (SykLB-YpY), or both (SykLB-pYpY). Changes in the ^{15}N-heteronuclear single-quantum coherence (HSQC) NMR spectrum of ^{15}N-labeled Vav1 SH2 upon titration with phosphorylated peptides were used to monitor the binding process.

NMR Lineshape Changes Reflect Relative Affinity. ^{15}N-HSQC spectra of Vav1 SH2 titrated with either SykLB-pYpY or SykLB-YpY are overlaid for each titration point in Figures 2A and 2B, respectively; the overlays upon titration with SykLB-pYY are nearly identical to those of SykLB-pYpY. Several SH2 peaks have substantial shifts upon titration as a result of direct intermolecular contact and/or alteration of the SH2 conformational equilibrium upon phosphopeptide binding. The spectral changes upon titration of Vav1 SH2 depend on the phosphorylation state; the titration pattern corresponds to the fast-exchange limit on the chemical shift timescale for SykLB-YpY, while most peaks show intermediate to slow exchange behavior when SykLB-pYpY or SykLB-pYY binds. The disparate exchange behavior is illustrated for peaks from S708 and I709 amide resonances in Figure 2C; in the case of SykLB-YpY

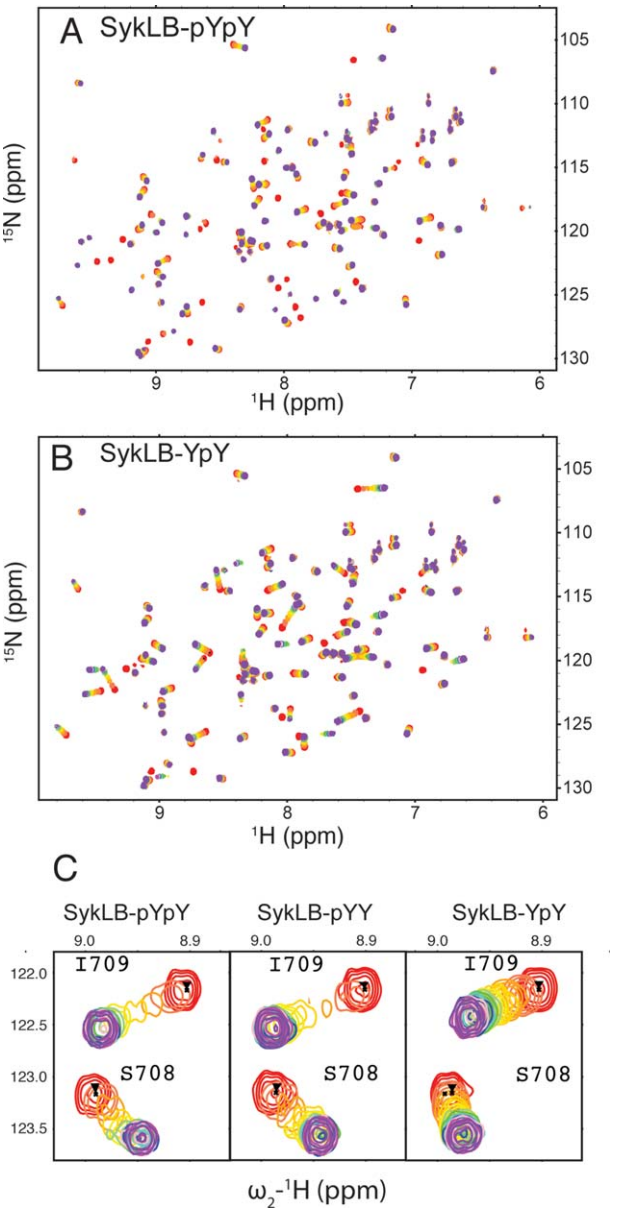

FIGURE 2 Titration of Vav1 SH2 with Syk-derived phosphopeptides monitored by ^{15}N-HSQC. Contours are colored as a rainbow from red, no ligand, to violet, saturating levels of ligand (see Methods for actual SH2:peptide ratios). (A) Titration with SykLB-pYpY, residues $DTEVpY_{342}ESPpY_{346}ADPE$. (B) Titration with SykLB-YpY, residues $DTEVY_{342}ESPpY_{346}ADPE$. (C) An expanded region showing S708 and I709 peaks during the titration with SykLB-pYpY, SykLB-pYY (residues $DTEVpY_{342}ESPY_{346}ADPE$), or SykLB-YpY showing intermediate and similar exchange behavior for SykLB-pYpY and pYY compared to the fast-exchange behavior for SykLB-YpY consistent with the binding affinities (SykLB-YpY $K_D = 71$ μM; SykLB-pYpY $K_D = 7.4$ μM; SykLB-pYY $K_D = 14.6$ μM).

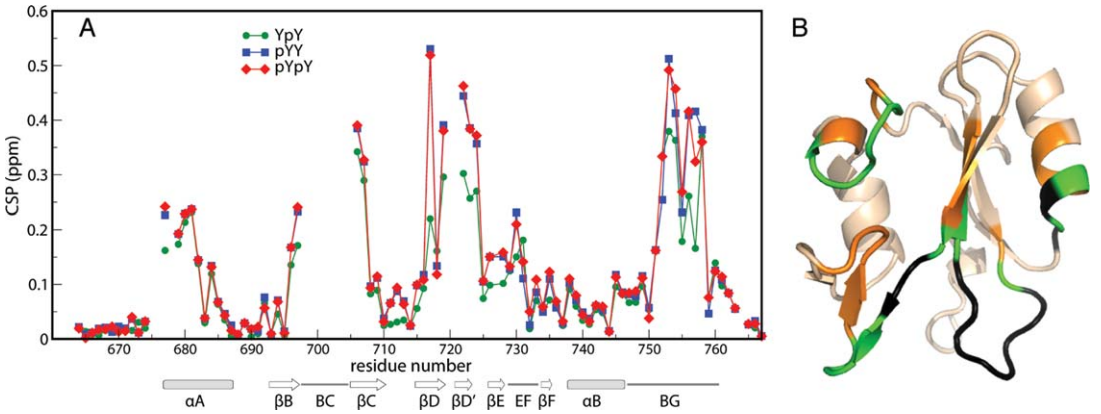

FIGURE 3 (A) CSP values plotted as a function of Vav1 SH2 residue number for titration with SykLB-YpY (green), SykLB-pYY (blue), or SykLB-pYpY (red) phosphopeptide. (B) Ribbon drawing of Vav1 SH2 domain (PDB code:2LCT) with large CSP values mapped to the structure: gold are residues with CSP > 0.15 ppm; green are large CSP values for which the SykLB-YpY complex value is smaller than the other two complexes; black are residues for which the resonance is missing in at least one of the three phosphopeptides complexes (residues 676, 678, 698:705, 720:721).

association (right panel), the S708 and I709 resonances are observed throughout the titration with SykLB-YpY with little change in linewidth, whereas in the case of both SykLB-pYpY and SykLB-pYY titrations (left and middle panels) the broadening and loss of peak intensity characteristic of intermediate exchange is evident. Given that the frequency difference between the free- and bound-state chemical shift is similar for the three peptides, these differences in exchange behavior are a direct indicator of faster pseudo-on/off rates and a lower binding affinity for SykLB-YpY relative to that for SykLB-pYpY and SykLB-pYY. The NMR exchange results are fully consistent with the kinetic rates and equilibrium constant for binding obtained using surface plasmon resonance measurements reported previously.[25] The affinity of SykLB-YpY is approximately 10-fold and 5-fold lower than the affinity of SykLB-pYpY and SykLB-pYY, respectively (SykLB-YpY $K_D = 71$ μM; SykLB-pYpY $K_D = 7.4$ μM; SykLB-pYY $K_D = 14.6$ μM). Based on NMR exchange dynamics,[27,28] a switch from fast-exchange to intermediate-exchange behavior, for a resonance with roughly the same total change in frequency upon binding two ligands, corresponds to approximately an order of magnitude difference in K_D, as observed for Vav1 SH2.

Residue Profiles of CSP for Binding SykLB-pYpY, SykLB-pYY, and SykLB-YpY. The association of the Syk phosphopeptides with Vav1 SH2 leads to large-magnitude changes in the ^{15}N-HSQC chemical shifts. CSP calculated from the difference in resonance frequency of the unligated and bound states as described in Material and Methods, are plotted for each SH2 residue in Figure 3A. The pattern of the residue profiles has four regions showing large perturbations greater than 0.2 ppm, and is remarkably similar for the three complexes. Indeed, the CSP values upon binding SykLB-pYpY (red symbols) and SykLB-pYY (blue symbols) are nearly identical, while the profile for the lower-affinity SykLB-YpY complex (green symbols) is similar but somewhat smaller in magnitude for the four regions of high CSP. Large CSP values occur for residues lining the pTyr pocket (N-terminus of the αA helix, the two ends of the BC loop), the central β-sheet (βC, βD), the specificity pocket (BG loop), and parts of the secondary β-sheet (βD′ strand to the EF loop). The correspondence in the CSP profiles infers the differentially phosphorylated peptides have common binding surfaces and that the overall mode of binding is similar.

To visualize the CSP profiles, the values greater than 0.15 ppm are mapped onto the Vav1 SH2 structure in Figure 3B; orange represents residues with large CSP values common to all three complexes, green represents those for which the SykLB-YpY complex value is smaller relative to that for the SykLB-pYpY and SykLB-pYY complex, and black represents regions for which resonances are missing in one or more of the phosphopeptides complexes. Whereas the near equivalence in CSP values for the SykLB-pYpY/ and SykLB-pYY/Vav1 SH2 complexes suggest the bound conformation of these two phosphorylation states are highly similar, the residues mapped in green are regions with potential differences in the SykLB-YpY-bound complex to accommodate the combination of phosphorylated pY346 and unphosphorylated Y342.

Examination of Figure 3B finds that resonances with smaller magnitude CSP for the SykLB-YpY complex relative to

Table I Structural Statistics of 20 Final Structures

NOE Distance Restraints		
Protein NOE		
Total	2508	
Short range (li-jl $\leq$ 1)	1104	
Medium range (1 < li-jl < 5)	478	
Long-range (li-jl $\geq$ 5)	925	
Intermolecular NOE	26	
Dihedral angle restraints from TALOS	134	
RMSD (Å) to mean coordinates	Backbone	Heavy Atoms
Complex[a]	1.65 ± 0.33	2.15 ± 0.29
SH2 domain residues 664–697, 706–767	0.52 ± 0.09	1.10 ± 0.11
Peptide residues 341–347	0.92 ± 0.28	1.44 ± 0.32
Ramanchandran plot (%)		
Most favored regions	68.6	
Additionally allowed regions	25.3	
Generously allowed regions	4.0	
Disallowed regions	2.1	

[a] Vav1 SH2 residues 661–767 and YpY residues 338–350.

the other two complexes (green) are from residues that are, for the most part, in loops. In addition, the regions with exchange-broadened resonances in the ^{15}N-HSQC spectrum (black in Figure 3B) are flanked by residues with relatively smaller magnitude CSP, and two of these "hidden" regions mapped in Figure 3B have no direct contact with the SykLB-pYpY peptide[25]; these are in the BC loop, and between βD and βD′. In the case of the SykLB-pYpY/Vav1 SH2 complex, there is a conformational change in the secondary β-sheet and EF loop upon binding. Moreover, this region shows an unusual increase in mobility in the presence of the peptide; residues M721 and T722 were found to exhibit microsecond-to-millisecond motions in the SykLB-pYpY-bound state but not in the unbound state.[25] The sequential proximity of residues with relatively smaller SykLB-YpY CSP values to exchange-broadened residues that are distant from the binding site suggests that the CSP in these regions results from a change in conformational dynamics, as opposed to direct interaction with the peptide, and that the structural differences of the lower-affinity SykLB-YpY complex are also linked with SH2 regions of internal mobility.

NMR Structure of the Vav1 SH2/SykLB-YpY Complex

Solution Structure Determination. To better understand effects of differential phosphorylation of Syk Y342/346 on Vav1 interaction, we determined the structure of Vav1 SH2 in complex with SykLB-YpY using nOe-derived distance restraints and TALOS-derived main chain dihedral angle restraints in molecular dynamics simulations. The final complex structures were calculated with 2,508 intramolecular SH2 distance restraints obtained from iterative automatic assignment using CYANA, and 26 intermolecular distance restraints assigned manually between the Vav1 SH2 domain and the SykLB-YpY peptide. The majority of the intermolecular NOEs occur for peptide residues including and around Y342 and pY346: Y342 has nine nOe's; P345 has six nOe's; pY346 has four nOe's; and A347 has four nOe's. SykLB-YpY residues 343 and 344, between the two closely spaced tyrosines, have no intermolecular nOe's. A similar finding occurred for the SykLB-pYpY

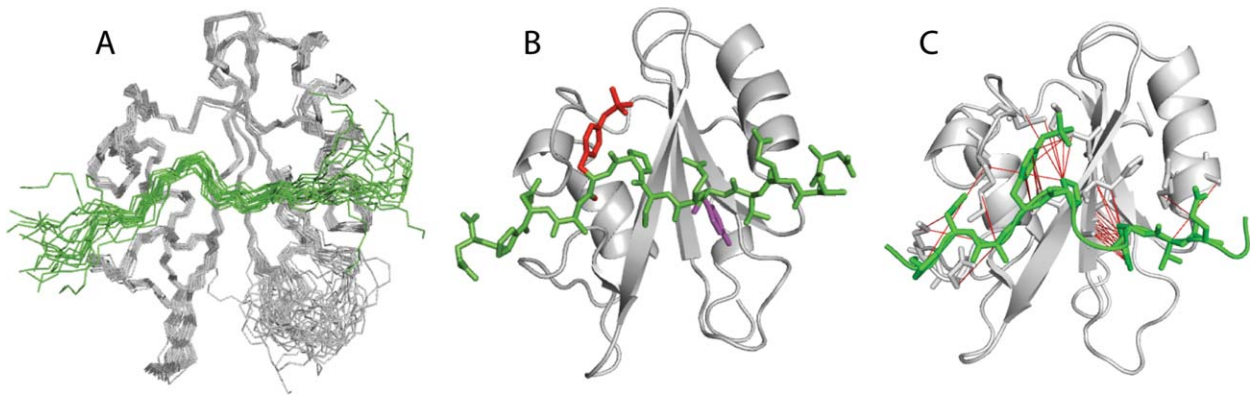

FIGURE 4 (A) set of 20 lowest-energy structures determined from NMR-restrained MD of the Vav1 SH2-YpY complex. Structures are represented by a main chain trace of SH2 (grey) and SykLB-YpY (green), and superimposed based on main chain atoms of the central β-sheet. (B) Ribbon drawing of the average structure obtained by averaging coordinates from the set of twenty structures, followed by energy minimization. The SykLB-YpY peptide is green. Y342 (purple) occupies the pTyr pocket, and pY346 (red) the specificity pocket. (C) Intermolecular nOe interactions visualized with lines between the SykLB-YpY protons and Vav1 SH2 protons.

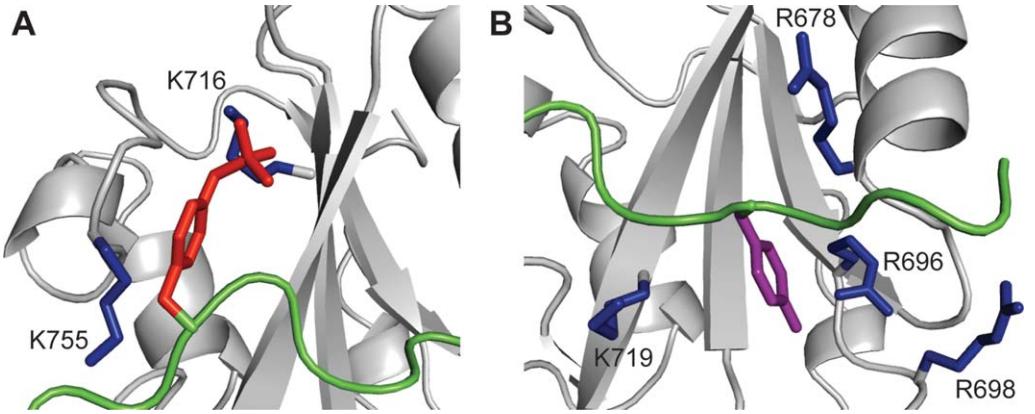

FIGURE 5 Ribbon representation in close-up view of the two binding pockets of Vav1 SH2 (grey) ligated with SykLB-YpY (green). (A) The specificity pocket occupied by phosphorylated pY346 (red sticks). K716 and K755 are highlighted with sticks. The key interaction for recognition of phosphotyrosine in the specificity pocket is with K716. (B) The pTyr pocket occupied by unphosphorylated Y342 (purple sticks). Important residues are shown with blue sticks.

complex of Vav1 SH2 where only one intermolecular nOe was observed for these residues of the peptide.[25] Structural statistics for 20 final structures for the SykLB-YpY-bound state are shown in Table I. The root mean square deviation (RMSD) corresponding to the ordered regions in the Vav1 SH2 domain (residues 664–697 and 706–767) is 0.52 ± 0.09 Å for the backbone and 1.10 ± 0.11 Å for heavy atoms. The RMSD for the well-ordered region of the SykLB-YpY peptide, residues 341–347, is 0.92 ± 0.28 Å for the backbone and 1.44 ± 0.32 Å for heavy atoms. This level of precision achieved from the NMR restraints is sufficient to allow a reliable description of the interactions between the Vav1 SH2 domain and the SykLB-YpY peptide.

Vav1 SH2/SykLB-YpY Complex Structure and Recognition. The set of 20 lowest-energy structures of the Vav1 SH2/SykLB-YpY complex is shown in Figure 4A, and the energy-minimized average structure in panel B. In the SykLB-YpY-bound state, the Vav1 SH2 domain retains the well-known topology with a central β-sheet followed by a smaller secondary β-sheet, both flanked by two α helices, and the SykLB-YpY peptide crosses the edge of the β-sheet (green in Figures 4A and 4B). The BC loop is unstructured (Figure 4A) given that the resonances for atoms in the BC loop are not observed, and therefore, without restraints in the MD simulations. The BC loop was similarly disordered in the case of the Vav1 SH2-SykLB-pYpY complex.[25]

A key point of the SykLB-YpY interaction with Vav1 SH2 is that pY346 (red, Figure 4B) binds the specificity pocket on the side of the central β-sheet opposite to the canonical pTyr-binding pocket, while the unphosphorylated Y342 (purple, Figure 4B) inserts into the canonical pTyr binding pocket. Consistent with the intermolecular nOe's illustrated in Figure 4C, most of the intermolecular contact derives from Y342 and pY346, plus P345 that matches the proline at (p)Tyr +3 in the consensus sequence. The intervening residues E343 and S344 crossing the central β-sheet have little direct interaction with Vav1 SH2. Two residues upstream of Y342, E340 (1 nOe), and V341 (1 nOe), make weak contact with the N-terminal end of the αA helix. These two residues also form intermolecular interactions in the SykLB-pYpY complex, and thus likely stabilize the orientation of the bound peptide with Y342 in the pTyr pocket whether or not phosphorylated. These upstream contacts are missing in the Vav1 SH2 complex with the pY128 peptide derived from SLP-76 (PDB code 2ROR).

Figure 5 is a detailed view of pY346 (panel A) and Y342 (panel B) interactions with Vav1 SH2. Instead of occupying the canonical pTyr pocket, pY346 binds the specificity-determining region on the left side of the β-sheet as viewed in Figure 5A. The phosphate group of pY346 interacts with the positively charged ε-amino groups of K716 in the βD3 position. A lysine residue occurs at the βD3 position in all SH2 domains known to have the ability to bind to the doubly phosphorylated peptide derived from Syk linker B,[1,16] and thus the Vav1 SH2/SykLB-YpY structure further emphasizes the importance of this recognition feature for the two-closely spaced tyrosine residues in Syk linker B. In addition to the phosphoryl group interactions, the aromatic ring of pY346 involves hydrophobic contact with the aliphatic portion of the K719 side chain in the second binding pocket.

For association in the pTyr pocket (Figure 5B), the aromatic ring of Y342, without the phosphoryl group, is closer

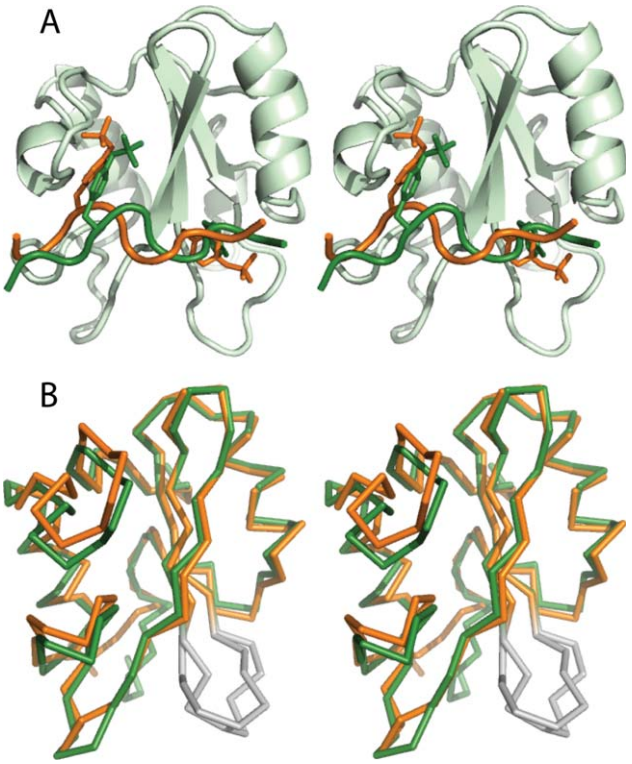

FIGURE 6 (A) Stereo-view of Vav1 SH2 phosphopeptide complexes in cartoon representation comparing the position of SykLB-YpY (green) and SykLB-pYpY (gold) on the protein surface. Tyrosine and phosphotyrosine residues of the peptide are in stick representation. The protein model is from the SykLB-YpY-SH2 complex. (B) Comparison of the SH2 domains from the SykLB-YpY (green) complex and the SykLB-pYpY (orange) complex. The BC loop is colored in grey to indicate resonances from this loop are not observed, and therefore, the loop is disordered.

to the universally conserved R696 on the βB strand compared to the contact in the SH2-SykLB-pYpY complex. Unphosphorylated Y342 has contact with R678 (αA2), R696 (βB5), R698, and K719 (βD6).

SykLB-YpY versus SykLB-pYpY Recognition. Comparison of the Vav1 SH2 structures in complex with either SykLB-YpY or SykLB-pYpY[25] finds that although the two peptides bind in the same general orientation and with each of the two closely spaced tyrosine residues in the same binding pockets of the Vav1 SH2 domain (Figure 6A), the specific positioning and intermolecular interactions differ. Without the phosphate group on Y342, this tyrosine lies in closer proximity to the βB strand and the conserved Arg696 such that the overall position of the SykLB-YpY peptide is shifted toward the αA helix relative to that of the SykLB-pYpY peptide. This shift appears to propagate along the SykLB-YpY chain in that pY346 is drawn toward the central β-sheet, and does not interact with K755 in the BG loop. In contrast, pY346 in the SykLB-pYpY-bound complex forms salt bridges with both K755 and K716. For the SykLB-YpY complex, the phosphoryl group of pY346 has larger solvent-accessible surface area than in the SykLB-pYpY complex and solvent must contribute some level of stabilization.

The different peptide position arising from no phosphorylation on Y342 in the SykLB-YpY complex compared to the SykLB-pYpY complex is accommodated by alternative conformations in the specificity pocket of Vav1 SH2 rather than the pTyr pocket. The differences, illustrated with a trace of the two complexes after aligning the structures by the central β-sheet of Vav1 SH2 in Figure 6B, are in the BG loop and the secondary β-sheet region including the EF loop. The canonical pTyr binding pocket retains almost the same conformation to bind either phosphorylated or nonphosphorylated Y342. This observation of the specificity pocket being the region of plasticity and the pTyr pocket being relatively unchanged was also made upon comparison with Vav1 SH2 binding the pY128 peptide derived from SLP-76.[25] The conformational changes in the specificity pocket alter the pocket dimension and thus can accommodate repositioning of the peptide for SykLB-YpY versus SykLB-pYpY or can accommodate the alternative sequences for pY128 versus linker B.

The conformational adjustments for binding the singly phosphorylated SykLB-YpY generate an electrostatic potential surface of the SH2 domain to complement the reduced negative charge of the peptide. The electrostatic potential calculated with the DelPhi program[29] is mapped to the surface of the SykLB-pYpY complex in Figure 7A and the SykLB-YpY complex in Figure 7B. Both binding sites are positively charged, but changes in the conformation of K755 in the BG loop and R698 in the BC loop result in a relatively less electropositive potential surface in association with SykLB-YpY.

DISCUSSION

Differential Recognition of Phosphotyrosine and Syk Linker B-Mediated Antigen Signaling in B Cells

In contrast to the vast number of existing structures of SH2-phosphopeptide complexes, the solution structure of the Vav1 SH2 complex with the singly phosphorylated peptide SykLB-YpY derived from Syk linker B shows that phosphorylated Y346 binds the specificity pocket rather than the pTyr pocket typically occupied by phosphotyrosine. This atypical, "swapped" binding mode exists even though the sequence C-terminal to pY346 of SykLB-YpY (DTEVY$_{342}$ESPpY$_{346}$ADPE) matches the consensus recognition sequence pYΦXP for Vav1 SH2,[17,30] and would, therefore, be predicted to bind the pTyr pocket. The experimental evidence that establishes this atypical

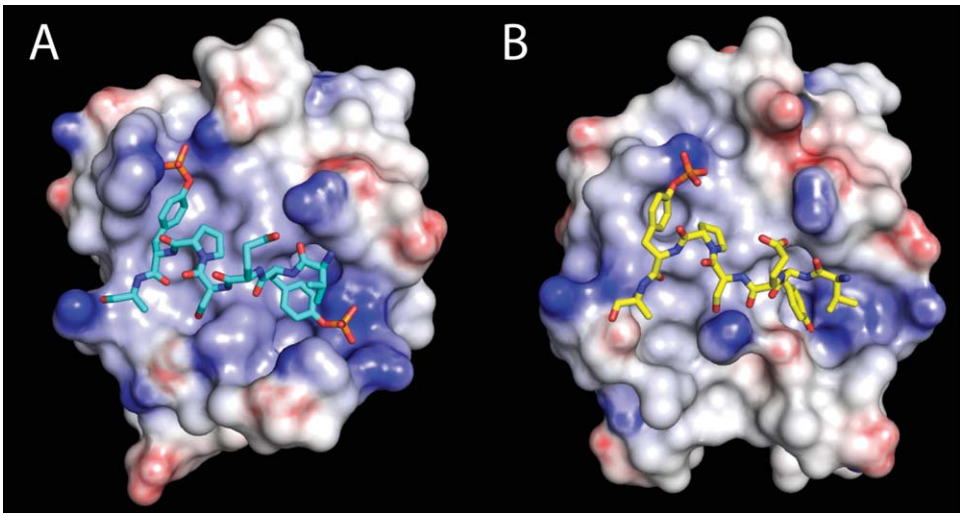

FIGURE 7 Electrostatic potential of the Vav1 SH2 domain in the complex with (A) SykLB-pYpY or (B) SykLB-YpY, calculated with the DelPhi program and mapped by color onto the surface of the protein. Darker blue corresponds to increasingly positive charge, and darker red to increasingly negative charge.

binding mode is the unambiguous intermolecular nOe interactions of Y342 and pY346 with Vav1 SH2 (Figure 4C), and the nearly identical CSP profiles (Figure 2) upon binding SykLB-YpY or SykLB-pYpY. That is, in the known structure of Vav1 SH2/SykLB-pYpY, pY346 binds the specificity pocket and pY342 is positioned in the canonical pTyr pocket,[25] and thus the close similarity of the CSP profile of SykLB-YpY indicates the same overall binding orientation of the phosphopeptides on the surface of Vav SH2.

The results reported here provide a structural framework to understand how linker B phosphorylation of the two closely spaced tyrosines mediates Syk interactions with Vav as well as other proteins critical to B cell signaling.[1] The linker B-mediated association of Syk with Vav proteins leads to Syk phosphorylation of Vav on tyrosines that regulate Vav activity.[31–33] An important point is that the relative binding affinity of Vav1 SH2 for the doubly and two singly phosphorylated forms correlates with the cellular response levels in B cell signaling measured by nuclear factor of activated T-cells, NFAT, activation.[25] Importantly, this differential response of cells indicates all three phosphorylation states of Syk linker B Y342/Y346 function in the cell, and the swapped mode of phosphotyrosine binding to the specificity pocket of Vav plays a role in signaling. Tuning the affinity of the Syk-Vav association through phosphorylation of Y342 and Y346 affects the competition for Syk among multiple Syk-binding proteins, and possibly determines cellular response by modulating the flux through alternative signaling pathways.

This control of B cell signaling is associated with small changes in the affinity of the Vav-Syk interaction. The effect of a single tyrosine phosphorylation of Syk linker B on either Y342 or Y346 is to promote binding to Vav1 SH2, with approximately five times higher affinity for Y342 phosphorylation relative to that for Y346. A second phosphorylation event further increases affinity; in the presence of pY346 generation of the doubly phosphorylated docking site with pY342 and pY346 enhances affinity 10-fold, but has only a two-fold increase in affinity when Y342 is already phosphorylated. Overall, these modest differences in affinity correlate with cellular response levels of B cells.[25]

The differential recognition of Y342 and Y346 by both the specificity pocket and the pTyr pocket of Vav1 SH2 provides a mechanism to enable association of multiple binding partners, a fundamental component of cellular signaling networks. The complex of Vav1 SH2 with SykLB-YpY described here and the simultaneous binding of the two closely spaced phosphotyrosines pY342 and pY346 to SH2 reported previously for Vav1[25] and PLC-γ[16] together find that the phosphoryl group in the specificity pocket interacts with the side chain amino group of Lys at the βD3 position. In addition, a Lys residue occurs at this position in all other SH2 domains that bind the doubly phosphorylated form of Syk at Y342 and Y346,[16] and thus this interaction appears to be a key recognition determinant for phosphotyrosine binding the specificity pocket of SH2 domains. This recognition of phosphotyrosine by the specificity pocket of SH2, with no dependence on phosphotyrosine binding the pTyr pocket, raises the intriguing possibility that various proteins

with such SH2 domains have the ability to recognize a second subset of binding partners mediated by the specificity pocket.

Peptide-induced conformational changes occur in the specificity pocket, while the pTyr pocket remains relatively unchanged in conformation. There are small shifts in the main chain of the secondary β-sheet and the BG and EF loops to accommodate small differences in the orientation of the SykLB-YpY peptide compared to SykLB-pYpY. These changes in the BG and EF loops reflect the important role of loops in conferring specificity of SH2 domains previously noted.[34] Thus, the phosphorylation state of Y342 determines the specific position of tyrosine in the pTyr pocket, yet the adjustment in SH2 conformation to accommodate this positioning is found to occur remotely in the specificity pocket. The secondary β-sheet and the BG and EF loops are also the regions of Vav1 SH2 that exhibit mobility based on N_H transverse relaxation,[25] so that as expected, the flexible regions of the SH2 domain are the more adaptive ones.

Phosphotyrosine-Independent Binding in the pTyr Pocket

Phosphotyrosine-independent binding to SH2 has been reported for two other SH2 domains, SAP and tensin2[22,23,35,36] and structurally characterized for SAP,[22,23] but to the authors' knowledge, the Vav1 SH2 recognition of Syk SykLB-YpY is the first observation of an unphosphorylated tyrosine binding the pTyr pocket when the peptide ligand also contains a recognizable phosphorylated tyrosine.

In the complete absence of phosphotyrosine, unphosphorylated tyrosine binds the pTyr pocket of SAP,[22,23] a single SH2-domain protein that recognizes the signaling lymphocyte activation molecule, SLAM, and is associated with X-linked lymphoproliferative syndrome. Unphosphorylated and phosphorylated peptides derived from SLAM adopt essentially the same bound conformation in association with SAP SH2.[23] Residues N-terminal to the tyrosine interact with protein in unphosphorylated SAP SH2 complexes[22,23] and are present as well as in the Vav1 SH2/SykLB-YpY complex. These additional contacts, beyond the characteristic C-terminal residue interactions, may help to stabilize the unphosphorylated tyrosine binding.

For SAP and tensin2 SH2 that bind tyrosine independent of phosphorylation, the affinity for unphosphorylated tyrosine is reduced less than 10-fold relative to the analogous phosphorylated peptide.[22,23,36] Vav1 SH2 affinity difference of SykLB-YpY and SykLB-pYpY is 71 μM versus 7.4 μM, and thus, the stabilization contributed by the phosphoryl group in the pTyr pocket is only ~1.4 kcal/mol. In contrast, for Src SH2 the binding of phosphotyrosine in the pTyr pocket can contribute as much as half of the total binding free energy based on results from isothermal titration calorimetry studies,[21,37] and attributing near half of the binding free energy to phosphorylation of tyrosine is sometimes considered a general property of SH2 domains.[18] Nevertheless, the analysis of Vav1 reported here, as well as the previous reports for SAP and tensin2 SH2 domains, demonstrate that the phosphoryl group alone can contribute considerably less of the total binding energy depending on the particular SH2 interaction.

CSP and Binding Affinity

The magnitude of CSPs is sometimes found to be proportional to binding affinity[38] or binding enthalpy.[39] Clearly, such a correlation is not a general one in that the physical basis for such a correlation is limited to comparisons in which it is reasonable that the binding energetics can be linearly related to chemical shift. As an example where affinity is not reflected in the magnitude of the chemical shift changes, PLC-γ SH2 binds the same Syk-derived peptides examined here but with 100–1000 times higher affinity than Vav1 SH2, yet the CSP values for PLC-γ SH2 are quite small; no CSP value is greater than 0.2 ppm, and only about 10 are greater than 0.1 ppm.[16] Nonetheless, for similar ligands binding to a given protein, or the same ligand to mutant proteins, a high correlation between CSP magnitude and affinity can be observed.

A remarkable similarity in the CSP profile of Vav1 SH2 for binding SykLB-YpY, SykLB-pYpY, and SykLB-pYY was observed (Figure 3A). Further, the profiles show a correspondence between affinity and CSP magnitude; the reduced affinity of SykLB-YpY relative to SykLB-pYpY and SykLB-pYY corresponds to somewhat smaller magnitude CSP for a few resonances in the SykLB-YpY complex. Of interest is that most of these resonances with smaller magnitude CSP are from residues in high-mobility loop regions of Vav1 SH2 (i.e., in Figure 3B, the residues mapped in green are adjacent to the black regions). This behavior suggests the equilibrium between different conformations separated by low free-energy barriers is somehow linked to the binding energetics and contributes to the differences in binding affinity. Although the mechanism is not established for how the internal motion of these loop regions could contribute to binding, the premise is nonetheless consistent with the fact that the differences in affinity are reflected in the on rates for binding rather than the off rates.[25]

MATERIAL AND METHODS

NMR Sample Preparation and Titration

The ^{15}N-labeled Vav1 SH2 sample was expressed and purified using the protocol described in the Ref. 25. The protein was in Tris buffer

containing 20 m*M* Tris at pH 7.0, 100 m*M* NaCl, 1 m*M* DTT, and 0.02% NaN_3. The pure phosphopeptides, SykLB-pYpY, SykLB-pYY, and SykLB-YpY, were purchased from EZBiolab. The concentration of the doubly phosphorylated peptide, SykLB-pYpY, was measured using an extinction coefficient of 1304 $M^{-1}cm^{-1}$ at 267 nm, based on an extinction coefficient for phosphotyrosine of 652 $M^{-1}cm^{-1}$.[40] For the singly phosphorylated peptides, SykLB-pYY and SykLB-YpY, the extinction coefficient is 2079 $M^{-1}cm^{-1}$ at 267 nm which represents the sum of extinction coefficients for tyrosine and phosphotyrosine.[41]

The ^{15}N-labeled Vav1 SH2 protein samples were prepared at 0.2 mM in 550 µl with 10% D2O. All titration experiments were performed at 298 K on a Bruker Avance-III-800 spectrometer. A series of sensitivity-enhanced ^{1}H-^{15}N HSQC spectra for the sample at different protein-peptide ratios were collected with eight scans and 1024 (^{1}H) × 64 (^{15}N) complex points. The titration experiments were done at protein-peptide molar ratios of 1:0, 1:0.15, 1:0.29, 1:0.44, 1:0.58, 1:0.73, 1:0.88, 1:1.17, 1:1.46, 1:2.04, 1:2.92, 1:4.67 for the SykLB-pYpY peptide; 1:0, 1:0.15, 1:0.30, 1:0.44, 1:0.59, 1:0.74, 1:0.89, 1:1.18, 1:1.48, 1:2.07, 1:3.25, 1:5.61 for the SykLB-pYY peptide; 1:0, 1:0.17, 1:0.34, 1:0.51, 1:0.68, 1:0.85, 1:1.02, 1:1.35, 1:1.69, 1:2.37, 1:3.72, 1:6.43 for the SykLB-YpY peptide.

CSP quantifies the chemical shift change upon binding to the peptide, and calculated as

$$\mathrm{CSP} = \sqrt{\frac{1}{2}\left[\Delta\delta H^2 + \left(\frac{\Delta\delta N}{5}\right)^2\right]}$$

where $\Delta\delta H$ and $\Delta\delta N$ are the chemical shift differences between the free and bound states in the proton and nitrogen dimensions, respectively.

NMR Structure Determination

Except the backbone amide assignments which were carried out from the titration, the structure of the SykLB-YpY-bound Vav1 SH2 complex was determined using the same protocol described in the Ref. 25. Briefly, intraprotein nOe's in simultaneous $^{15}N/^{13}C$-NOESY-HSQC and aromatic ^{13}C-NOESY-HSQC were assigned by CYANA 2.1.[42] Mainchain φ and ψ dihedral angle restrains were predicted using the program TALOS+ based on the chemical shifts of Cα, Cβ, Hα, and HN.[43] Twenty six nOe resonances in the 3D ($^{13}C/^{15}N$)-filtered ^{13}C-edited NOESY-HSQC spectrum were manually assigned. The complex structures were calculated and refined with XPLOR-NIH.[44]

The authors thank the Purdue University Interdepartmental NMR Facility (PINMRF) for NMR support. C.C. was supported by a Purdue Research Foundation Fellowship. Coordinates for the Vav1 SH2/SykLB-YpY complex have been deposited in the Protein Data Bank with accession code 2MC1.

REFERENCES

1. Geahlen, R. L. Biochim Biophys Acta Mol Cell Res 2009, 1793, 1115–1127.
2. Deckert, M.; TartareDeckert, S.; Couture, C.; Mustelin, T.; Altman, A. Immunity 1996, 5, 591–604.
3. DeFranco, A. L. Nat Immunol 2001, 2, 482–484.
4. Simon, M.; Vanes, L.; Geahlen, R. L.; Tybulewicz, V. L. J. J Biol Chem 2005, 280, 4510–4517.
5. Bustelo, X. R. Mol Cell Biol 2000, 20, 1461–1477.
6. Tybulewicz, V. L. J.; Henderson, R. B. Nat Rev Immunol 2009, 9, 630–644.
7. Katzav, S.; Sutherland, M.; Packham, G.; Yi, T. L.; Weiss, A. J Biol Chem 1994, 269, 32579–32585.
8. KonKozlowski, M.; Pani, G.; Pawson, T.; Siminovitch, K. A. J Biol Chem 1994, 271, 3856–3862.
9. Brooks, S. R.; Li, X. L.; Volanakis, E. J.; Carter, R. H. J Immunol 2000, 164, 3123–3131.
10. Marengere, L. E. M.; Mirtsos, C.; Kozieradzki, I.; Veillette, A.; Mak, T. W.; Penninger, J. M. J Immunol 1997, 159, 70–76.
11. Jevremovic, D.; Billadeau, D. D.; Schoon, R. A.; Dick, C. J.; Leibson, P. J. J Immunol 2001, 166, 7219–7228.
12. Gomez, T. S.; McCarney, S. D.; Carrizosa, E.; Labno, C. M.; Comiskey, E. O.; Nolz, J. C.; Zhu, P. M.; Freedman, B. D.; Clark, M. R.; Rawlings, D. J.; Billadeau, D. D.; Burkhardt, J. K. Immunity 2006, 24, 741–752.
13. Chiu, C. W.; Dalton, M.; Ishiai, M.; Kurosaki, T.; Chan, A. C. EMBO J 2002, 21, 6461–6472.
14. Jordan, M. S.; Sadler, J.; Austin, J. E.; Finkelstein, L. D.; Singer, A. L.; Schwartzberg, P. L.; Koretzky, G. A. J Immunol 2006, 176, 2430–2438.
15. Bohnenberger, H.; Oellerich, T.; Engelke, M.; Hsiao, H.-H.; Urlaub, H.; Wienands, J Eur J Immunol 2011, 41, 1550–1562.
16. Groesch, T. D.; Zhou, F.; Mattila, S.; Geahlen, R. L.; Post, C. B. J Mol Biol 2006, 356, 1222–1236.
17. Huang, H. M.; Li, L.; Wu, C. G.; Schibli, D.; Colwill, K.; Ma, S. C.; Li, C. J.; Roy, P.; Ho, K.; Zhou, S. Y.; Pawson, T.; Gao, Y. H.; Li, S. S. C. Mol Cell Proteomics 2008, 7, 768–784.
18. Liu, B. A.; Engelmann, B. W.; Nash, P. D. FEBS Lett 2012, 586, 2597–2605.
19. Bradshaw, J. M.; Mitaxov, V.; Waksman, G. J Mol Biol 1999, 293, 971–985.
20. Lindfors, H. E.; Drijfhout, J. W.; Ubbink, M. IUBMB Life 2012, 64, 538–544.
21. Ladbury, J. E.; Arold, S. T. In Methods in Enzymology; Michael L.; Johnson, J. M. H.; Gary, K. A., Eds.; Academic Press: New York, 2011; Chapter 7, pp 147–183.
22. Hwang, P. M.; Li, C.; Morra, M.; Lillywhite, J.; Muhandiram, D. R.; Gertler, F.; Terhorst, C.; Kay, L. E.; Pawson, T.; Forman-Kay, J. D.; Li, S.-C. EMBO J 2002, 21, 314–323.
23. Poy, F.; Yaffe, M. B.; Sayos, J.; Saxena, K.; Morra, M.; Sumegi, J.; Cantley, L. C.; Terhorst, C.; Eck, M. J. Mol Cell 1999, 4, 555–561.
24. Zhang, Y.; Zhang, J.; Yuan, C.; Hard, R. L.; Park, I.-H.; Li, C.; Bell, C.; Pei, D. Biochemistry 2011, 50, 7637–7646.
25. Chen, C. H.; Martin, V. A.; Gorenstein, N. M.; Geahlen, R. L.; Post, C. B. Mol Cell Biol 2011, 31, 2984–2996.
26. Hause, R. J., Jr.; Leung, K. K.; Barkinge, J. L.; Ciaccio, M. F.; Chuu, C. -P.; Jones, R. B. PLoS ONE 2012, 7, e44471.
27. Sandström, J. Dynamic NMR Spectroscopy; Academic Press: London, 1982.
28. Post, C. B. Methods Enzymol 1994, 240, 438–446.
29. Honig, B.; Nicholls, A. Science 1995, 268, 1144–1149.
30. Songyang, Z.; Shoelson, S. E.; McGlade, J.; Olivier, P.; Pawson, T.; Bustelo, X. R.; Barbacid, M.; Sabe, H.; Hanafusa, H.; Yi, T.;

Ren, R.; Baltimore, D.; Ratnofsky, S.; Feldman, R. A.; Cantley, L. C. Mol Cell Biol 1994, 14, 2777–2785.
31. Lopez-Lago, M.; Lee, K.; Cruz, C.; Movilla, N.; Bustelo, X. R. Mol Cell Biol 2000, 20, 1678–1691.
32. Miranti, C. K.; Leng, L.; Maschberger, P.; Brugge, J. S.; Shattil, S. J. Curr Biol 1998, 8, 1289–1299.
33. Moores, S. L.; Selfors, L. M.; Fredericks, J.; Breit, T.; Fujikawa, K.; Alt, F. W.; Brugge, J. S.; Swat, W. Mol Cell Biol 2000, 20, 6364–6373.
34. Kaneko, T.; Huang, H.; Zhao, B.; Li, L.; Liu, H.; Voss, C. K.; Wu, C.; Schiller, M. R.; Li, S. S. Sci Signal 2010, 3, ra34.
35. Liao, Y. -C.; Si, L.; White, R. W. D.; Lo, S. H. J Cell Biol 2007, 176, 43–49.
36. Dai, K.; Liao, S.; Zhang, J.; Zhang, X.; Tu, X. PLoS ONE 2011, 6, e21965.
37. Grucza, R. A.; Bradshaw, J. M.; Fütterer, K.; Waksman, G. Med Res Rev 1999, 19, 273–293.
38. Landry, S. J. Biochemistry 2003, 42, 4926–4936.
39. Ward, J. M.; Gorenstein, N. M.; Tian, J.; Martin, S. F.; Post, C. B. J Am Chem Soc 2010, 132, 11058–11070.
40. Grucza, R. A.; Futterer, K.; Chan, A. C.; Waksman, G. Biochemistry 1999, 38, 5024–5033.
41. Grucza, R. A.; Bradshaw, J. M.; Mitaxov, V.; Waksman, G. Biochemistry 2000, 39, 10072–10081.
42. Herrmann, T.; Guntert, P.; Wuthrich, K. J Mol Biol 2002, 319, 209–227.
43. Shen, Y.; Delaglio, F.; Cornilescu, G.; Bax, A. J Biomol NMR 2009, 44, 213–223.
44. Schwieters, C. D.; Kuszewski, J. J.; Tjandra, N.; Clore, G. M. J Magn Reson 2003, 160, 65–73.

Reviewing Editor: Alfred Wittinghofer